# A Mechanistic Approach to Modelling the Formation of a Drug Reservoir in the Skin

J.G. Jones[a,b,*], K.A.J White[a], M.B. Delgado-Charro[b]

[a] *Department of Mathematical Sciences, University of Bath, Bath BA2 7AY, UK*
[b] *Department of Pharmacy and Pharmacology, University of Bath, Bath BA2 7AY, UK*

**Abstract**

It has been shown that prolonged systemic presence of a drug can cause a build up of that drug in the skin. This drug 'reservoir', if properly understood, could provide useful and important information about recent drug-taking history of the patient. In this paper we create a pair of coupled mathematical models which combine together to explore the potential for a drug reservoir to be created based on the kinetic properties of the drug. The first compartmental model is used to characterise time-dependent drug concentrations in plasma and tissue following a customisable drug regimen. Outputs from this model provide boundary conditions for the second, spatio-temporal model of drug build-up and concentration profile in the skin.
We focus in particular on drugs that are highly bound as this will restrict their potential to move freely into the skin but which are lipophilic so that, in the unbound form, they would demonstrate an affinity to the outer layers of the skin (which are built around a lipid matrix). Buprenorphine, a drug used to treat opiate addiction, is one example of a drug satisfying these properties. In the discussion we highlight how our study might be used to inform future experimental design and data collection to provide relevant parameter estimates for reservoir formation and its potential to contribute to enhanced drug monitoring techniques.

*Keywords:* Skin, drug reservoir, binding, non-invasive drug monitoring, lipophilic, mathematical modelling.

## 1. Introduction

The reservoir function of the skin is a recognised phenomena in the field of percutaneous absorption [1]. A reservoir in the skin was first identified for the case of topically applied corticosteroids [2, 3] after a prolonged therapeutic effect was observed. Presence of a reservoir in the skin has since been demonstrated for many other drugs [1]. Moreover it has been shown, via tape stripping, that the main site of this skin reservoir is the stratum corneum (SC), the layer of dead cells at the skin surface [1, 2, 4].

Research on the presence of a reservoir in the SC is generally focussed on formation from an external source, specifically topically applied drugs and chemical exposure [1]; drug that comes

*Corresponding author
*Email addresses:* J.Jones2@bath.ac.uk (J.G. Jones), K.A.J.White@bath.ac.uk (K.A.J White), B.Delgado-Charro@bath.ac.uk (M.B. Delgado-Charro)

into contact with the skin surface enters the body via passive diffusion. As only unbound drug diffuses [5] the cause of a reservoir forming in the SC is thought to be high keratin binding and slow desorption kinetics [5]. Binding within the skin is most typical for lipophilic drugs with high molecular weight [6, 7].

More recently, detection of a 'reservoir' of drug in the skin as a result of systemic presence of that drug has highlighted the potential of skin to act as a site for noninvasive monitoring [8] both to measure systemic drug levels and to estimate historic usage by exploiting the reservoir.

The existence of such a reservoir in the SC has been demonstrated in the case of lithium [8, 9]. Lithium is a small drug which remains unbound and is not metabolised within the body. Mathematical modelling in that case [10], showed how the drug reservoir could be used to assess prescription compliance; but it was a simplest case scenario in many ways given the properties of the drug within the body.

The purpose of this paper is to extend that work to use a mathematical modelling approach to explore the potential for reservoir formation with a more complex drug. In particular, we are interested in a drug that is metabolised within the body; bound to molecules within the body; and lipophilic. These choices reflect the properties of many prescription drugs that are metabolised as well as excreted by the body and which bind to proteins and other molecules within both the plasma and the tissue. The choice of a lipophilic drug reflects the composition of the SC which consists of a lipid matrix together with corneocytes and their connecting structures, desmosomes; by focussing on a drug that is lipophilic, we assume that the drug will have affinity to the SC and potentially a tendency to accumulate in this outer skin layer. The drug buprenorphine used to treat opiate addiction, where compliance is an essential component of effective treatment, satisfies these three criteria and so acts as a motivation for our choice. Despite being well-established, parameter estimates for buprenorphine in the mechanistic model structure are not readily available from the literature and so we use this example simply as a motivation at this stage for our theoretical modelling work.

Classical modelling approaches to drug absorption, distribution, metabolism and excretion (ADME processes) often use a phenomenological approach in which model compartments represent theoretical spaces to give model predictions that fit well with the data. These are known as pharmacokinetic models. More recently, there has been a move towards more complicated physiologically based pharmacokinetic models (PBPK) which take a mechanistic approach, modelling each component of the body relevant to the passage of a given drug [11]. PBPK models are used as predictive tools in research, drug development and risk assessment. However, these models require large amounts of data to estimate the considerable number of model parameters.

In the following section we build the model structure which consists of two sub-models that couple together to provide a profile of compartmental drug concentrations in the body and spatial distribution within the SC. The compartmental body model is a simplified form of a PBPK model where we restrict the number of body compartments to three, invoking Occams razor. The outputs from this model provide boundary conditions for the spatial distribution model in the SC. Analysis of the models leads to predictions about the effect of bound and unbound plasma drug concentration, drug compliance, binding coefficients and diffusive potential on reservoir size. We conclude with observations about the potential to exploit the SC reservoir as a mechanism for non-invasive drug monitoring.

## 2. Model

The mathematical model is built in two stages: firstly, a compartmental system of coupled ODEs is used to model time-dependent drug concentrations within the body in response to a regularly administered drug. The outputs from this model provide boundary conditions for the second stage model which explores the spatial distribution of drug molecules within the SC; in turn, this is used to calculate the total amount of drug (the reservoir) within the SC as a function of key, critical parameters. It should be noted that whilst Model 1 feeds into Model 2, the converse is not true. We assume that any drug which enters the SC is not reabsorbed into the blood. We assume that active drug is administered and it is the administered drug that we are interested in modelling. A single daily dose is administered in the fully compliant case. For simplicity we will not consider drug-drug interactions.

### *2.1. Model 1*

This model comprises six time-dependent state variables: unbound drug molar concentration in plasma, $P_u(t)$; bound drug concentration in plasma, $P_b(t)$; unbound drug concentration in well perfused tissues, $Q_u(t)$; bound drug concentration in well perfused tissues, $Q_b(t)$;unbound drug concentration in poorly perfused tissues, $R_u(t)$ and bound drug concentration in poorly perfused tissues, $R_b(t)$ at time t. Noting that only unbound drug is able to move between plasma and tissue, we create a mathematical model based on the schematic shown in Figure 1. The model equations are built from conservation principles on the amount of drug in the system. For unbound drug in the plasma we have:

$$\begin{aligned} &\text{Change in amount of unbound drug in plasma (over time)} \\ &\quad = -\text{ net binding of drug to plasma proteins} \\ &\qquad -\text{ net movement of drug into well perfused tissues} \\ &\qquad -\text{ net movement of drug into poorly perfused tissues} \\ &\qquad -\text{ drug metabolised and excreted} \\ &\qquad +\text{ administered drug.} \end{aligned} \tag{1}$$

As we are considering a fixed plasma volume, $V_p$, the amount of drug in the plasma is $P_u(t)V_p$.

*(Net) Binding.* Binding in the plasma is a reversible process where, at equilibrium, unbound drug will be a fraction, $f_{up}$, of the total drug in the plasma, $(P_u + P_b)$. We assume that the rate at which this equilibrium is approached is directly proportional to the difference between the amount of unbound drug at time t, $P_u(t)$, and the amount that will be unbound at equilibrium, $f_{up}(P_u + P_b)$. This gives rise to a binding rate

$$-k_1(P_u - f_{up}(P_u + P_b)),$$

where $k_1$ is a positive rate constant. The effect of this term on the amount of unbound drug will be positive if $P_u$ is below its equilibrium level and negative if above.

*(Net) Movement Into Tissue.* Again, this process is reversible. Only unbound drug moves between plasma and tissue which we exploit to give the rate of movement into tissue from the plasma as

$$-k_2(P_u - f_2Q_u) - k_3(P_u - f_3R_u).$$

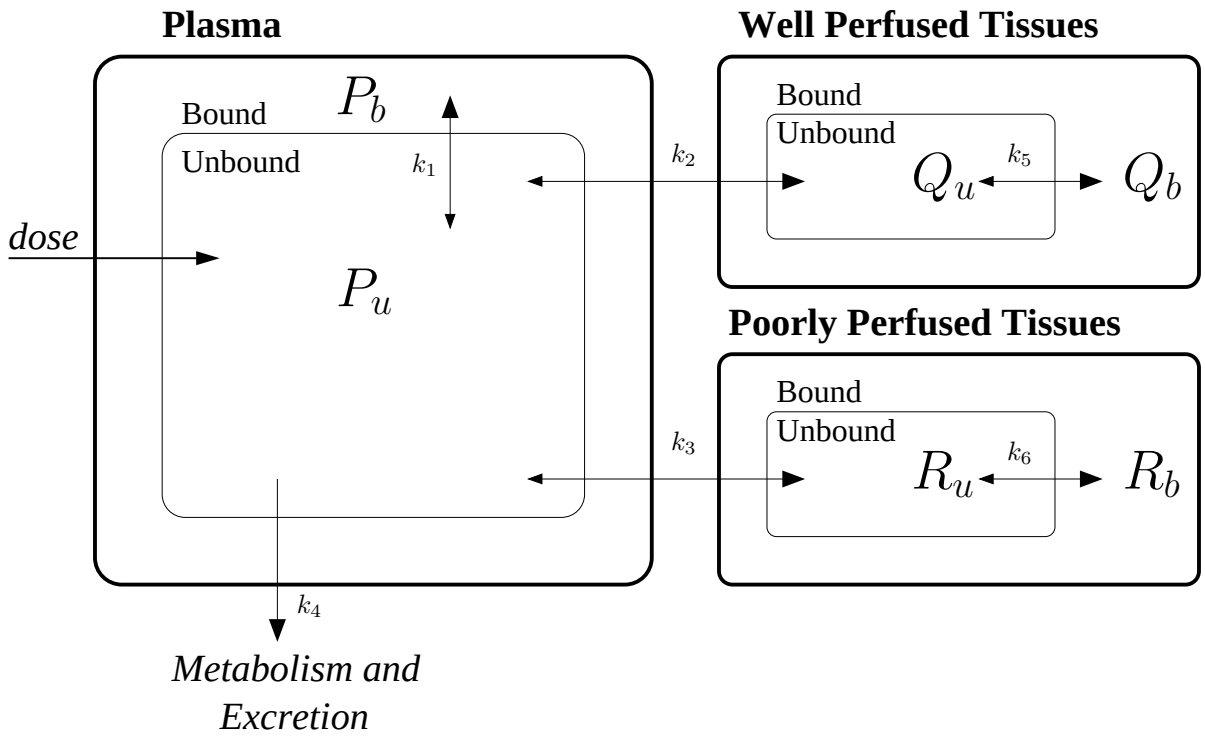


Figure 1: Schematic demonstrating the flow of drug within a simplified body compartmental structure. Parameters $k_i$ $(i = 1...6)$ are described in the text.

The parameters $k_2$, $k_3$ are the rates at which movement occurs and are dependent on a number of variables such as blood flow to tissues and partitioning coefficients.
Tissues are assigned to well perfused or poorly perfused tissue compartments according to blood perfusion values given in [12]. It therefore follows that $k_2 > k_3$. The remaining two parameters, $f_2$ and $f_3$ represent the ratio between concentration of drug in plasma and well perfused tissue, and plasma and poorly perfused tissue at equilibrium respectively. According to the allocation of tissues to each compartment, poorly perfused tissues have a much higher fat percentage than well perfused tissues [12]. As we are considering lipophilic drugs we can also expect $f_2 > f_3$ (higher affinity for fatty tissue).

*Metabolism.* Metabolism is described by Michaelis Menten kinetics. Only unbound drug in the plasma is metabolised. Hence we obtain the rate of metabolism:

$$\frac{V_{max} P_u}{k_m + P_u},$$

where $V_{max}$ and $k_m$ are the maximum velocity and michaelis constant respectively.

*Multiple Dose.* The term describing administration of drug is of the form

$$\sum_{i=1}^{N} \delta k \exp(-k(t - T_i))$$

as used in the model by Paulley et al [10] for a repeat lithium dose. For simplicity, on administration, dose is assumed to be distributed homogeneously in the plasma. The parameter $\delta$ is the 'size' of the dose that arrives in the body, calculated as the mass of dose $\times$ bioavailability and converted to molar concentration by dividing through by molar mass and plasma volume. The dissolution/ absorption rate constant for the given route of administration is given by $k$, which reflects that drug not given intravenously will not all arrive in the body immediately. Doses are administered at the times $T_i$ where $N$ is the number of doses administered [10, 13].

Combining these terms with (1) gives rise to the model equation

$$\begin{aligned}\frac{dP_u}{dt} =& - k_1(P_u - f_{up}(P_u + P_b)) - k_2(P_u - f_2 Q_u) - k_3(P_u - f_3 R_u) \\ & - \frac{V_{max} P_u}{k_m + P_u} - k_4 P_u + \sum_{i=1}^{N} \delta k \exp(-k(t - T_i)),\end{aligned}$$

where parameters and variables are defined as in Table B.1 (see appendix).
Note that $\int_{T_i}^{\inf} \delta k \exp(-k(t - T_i))dt = \delta$ which means that the full dose $\delta$ does eventually reach the plasma.

*Volume Adjustment Between Compartments.* We assume bound and unbound drug occupy the same volume within compartments. We can not, however assume that volume between compartments is the same. We introduce the dimensionless variables $v_{Q/P} = \frac{v_Q}{v_P}, v_{R/P} = \frac{v_R}{v_P}$ where $v_Q$, $v_P$ and $v_R$ are the volumes of $Q$, $P$, and $R$ respecitvely. This ensures that the conservation of mass is maintained as drug moves between compartments.

Combining all elements, we obtain the full model system:

$$\begin{aligned}\frac{dP_u}{dt} =& - k_1(P_u - f_{up}(P_u + P_b)) - k_2(P_u - f_2 Q_u) - k_3(P_u - f_3 R_u), \\ & - \frac{V_{max} P_u}{k_m + P_u} - k_4 P_u + \sum_{i=1}^{N} \delta k \exp(-k(t - T_i)), \qquad (2a)\end{aligned}$$

$$\frac{dP_b}{dt} = k_1(P_u - f_{up}(P_u + P_b)), \qquad (2b)$$

$$\frac{dQ_u}{dt} = k_2 v_{Q/P}(P_u - f_2 Q_u) - k_5(Q_u - f_{uQ}(Q_u + Q_b)), \qquad (2c)$$

$$\frac{dQ_b}{dt} = k_5(Q_u - f_{uQ}(Q_u + Q_b)), \qquad (2d)$$

$$\frac{dR_u}{dt} = k_3 v_{R/P}(P_u - f_3 R_u) - k_6(R_u - f_{uR}(R_u + R_b)), \qquad (2e)$$

$$\frac{dR_b}{dt} = k_6(R_u - f_{uR}(R_u + R_b)). \qquad (2f)$$

Using parameters described in Table B.1 (which are estimates for buprenorphine taken from the literature) and assuming no drug in all compartments initially, we obtain concentration profiles as shown in Figure 2 we use this profile as input to Model 2 where drug accumulates in the stratum corneum.

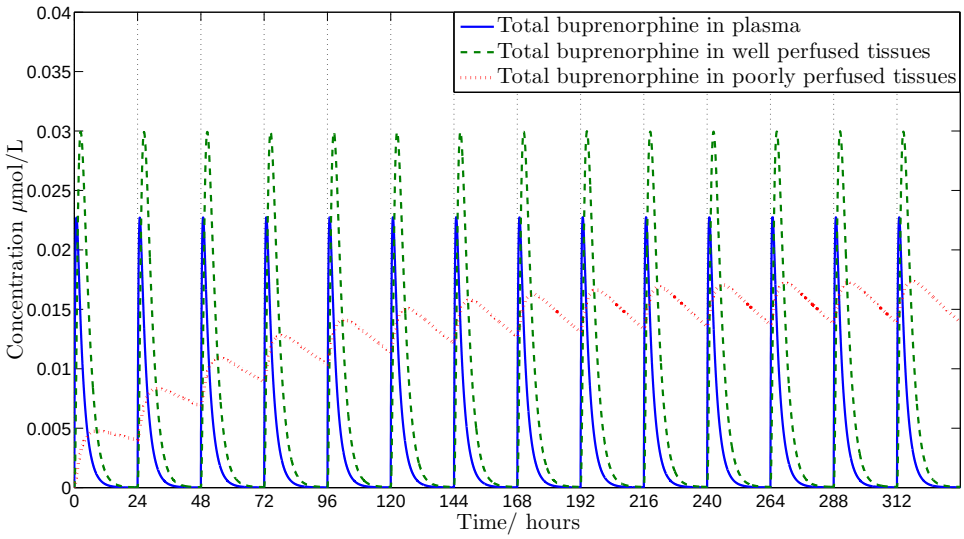


Figure 2: Simulation of plasma and tissue concentration profiles for a daily drug administration, using model 2 with parameter values as given in Table B.1.

### *2.2. Model 2*

In this section we obtain a description of the formation of a drug reservoir in the stratum corneum (SC). Our hypothesis is that drug builds up in the SC to create a reservoir where inflow from poorly perfused tissues is balanced by a loss from skin surface.

*Drug Binding in Skin.* In model 1, we considered bound and unbound drug in the plasma and tissues. Drug binds to keratin in the skin [7] and the dynamics of binding in the skin have been shown to be linear [14]. As only unbound drug is free to diffuse [5], binding may be an important factor in the formation of a SC reservoir. We therefore consider both bound and unbound drug in the SC and allow for the possibility of binding and unbinding.

*Passive Diffusion Through the Skin.* Movement of drug into the skin occurs via passive diffusion down concentration gradients and is described by Fick's law of diffusion assuming a constant diffusion coefficient, $D > 0$.

*Movement with the Differentiating Cells.* Cells and intercellular material in the skin move from the viable epidermis to the skin surface where they are shed [15, 16]. This movement is often neglected in delivery studies as the timescale under consideration is usually too short. However Simon et al included the effects of epidermal turnover in their mathematical drug delivery model [17]; in that case the epidermal turnover opposed movement of the drug into the SC from the skin surface. In this case we are considering the movement of drug from the base of the SC to the skin surface i.e. with the direction of movement of renewing cells. Epidermal turnover and desquamation is affected by many variables including hydration, time of day and skin condition. Here we focus on the underlying mechanism and assume that the skin moves towards the body surface at constant velocity $v > 0$.

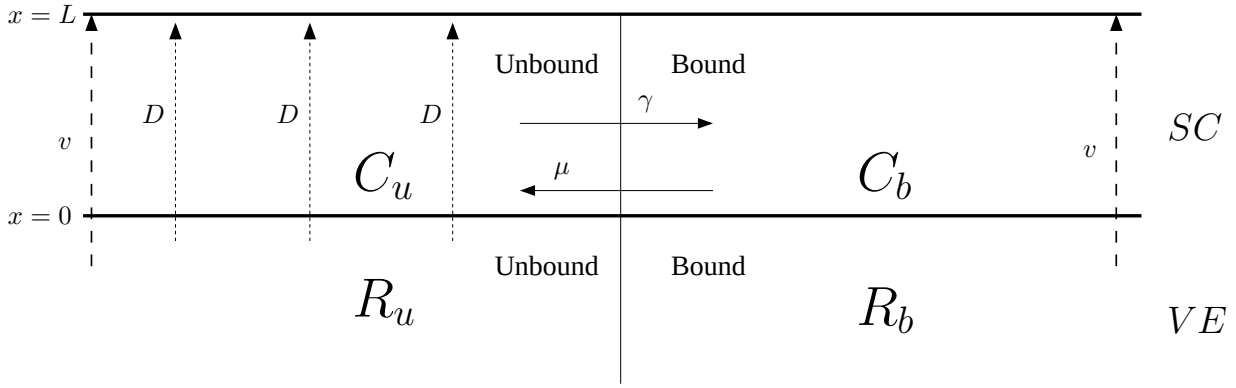


Figure 3: Schematic for model 2 where SC is the stratum corneum and VE is the viable epidermis represented by 'poorly perfused tissues' from model 1. Dotted arrows denote diffusion of unbound drug and dashed arrows denote convective movement of bound and unbound drug due to the renewal of the stratum corneum at rate $v$.

*Model Assumptions.* We consider a one-dimensional spatial domain for the SC since we assume that the drug is distributed homogeneously across the viable epidermis (VE), the layer below the SC. In this case $x = 0$ corresponds to the boundary between the SC and VE and $x = L$ corresponds to the surface of the skin.
We let $C_u(x,t)$ and $C_b(x,t)$ denote the concentration of unbound and bound drug at $x$ at time $t$ respectively and develop a diffusion-convection model based on the schematic shown in Figure (3) assuming that

1. Unbound drug diffuses across the SC with diffusion coefficient $D > 0$.
2. Bound and unbound drug move towards the surface of the skin at constant velocity $v > 0$ corresponding to the cell renewal in the SC.
3. Bound drug becomes unbound at the rate $\mu > 0$ and unbound drug becomes bound at rate $\gamma > 0$.
4. At $x = 0$, concentration of bound and unbound drug corresponds to those values obtained from the poorly perfused tissue in the compartmental model, $R_b(t), R_u(t)$ respectively.
5. At $x = L$, we assume no diffusion across the surface of the skin.

Combining these elements we obtain the model system:

$$\frac{\partial C_u}{\partial t} = D\frac{\partial^2 C_u}{\partial x^2} - v\frac{\partial C_u}{\partial x} + \mu C_b - \gamma C_u, \tag{3a}$$

$$\frac{\partial C_b}{\partial t} = -v\frac{\partial C_b}{\partial x} - \mu C_b + \gamma C_u. \tag{3b}$$

At $x = 0$, the interface between the stratum corneum and viable epidermis, the boundary conditions are

$$C_u(0,t) = \alpha R_u(t), \tag{4a}$$

$$C_b(0,t) = \alpha R_b(t), \tag{4b}$$

$$\tag{4c}$$

where $\alpha$ reflects a change in volume between poorly perfused tissues and the SC and where $R_u(t)$ and $R_b(t)$ are outputs from model 1. Boundary conditions at the surface are given by

$$D\frac{dC_u}{dx}\bigg|_{x=L} = 0 \qquad \text{(no diffusion across skin surface).} \tag{5}$$

*2.3. Calculation of Reservoir Size*

We consider the size of the reservoir to be the amount of drug across the entire thickness of the stratum corneum. If we consider constant boundary conditions $\alpha R_u(t) = \alpha\bar{R_u}$, $\alpha R_b(t) = \alpha\bar{R_b}$, we can find an expression for the drug distribution in the SC at steady state by setting the LHS of (3) equal to zero (for calculation see appendix Appendix A). This results in steady state distribution in the SC given by.

$$\underline{C} = a\underline{v}_0 + b\underline{v}_+ exp(\lambda_+ x) + c\underline{v}_- exp(\lambda_- x), \tag{6}$$

where $a, b$ and $c$ are constants, found using boundary conditions (4) to be

$$a = \alpha\bar{R_b} - b - c, \tag{7}$$

$$b = \left(\alpha\bar{R_u} - \frac{\alpha\mu\bar{R_b}}{\gamma} - \frac{cv\lambda_-}{\gamma}\right)\frac{\gamma}{\lambda_+ v}, \tag{8}$$

$$c = \frac{\alpha\left(\gamma\bar{R_u} - \mu\bar{R_b}\right)\left(\frac{\mu}{v} + \lambda_+\right)\exp(\lambda_+ L)}{\lambda_-[(\exp(\lambda_+ L)(\mu + \lambda_+ v) - \exp(\lambda_- L)(\mu + \lambda_- v)]}. \tag{9}$$

We use these distributions to explore the form and size of drug reservoir in the skin.

Note that if we consider binding and unbinding occurring at an equal rate ($\mu = \gamma$) and constant boundary conditions with equal concentrations of bound and unbound drug ($\alpha R_u = \alpha R_b$) then from equations (7-9) c=0 and so b=0 giving a=$\alpha R_b$. Using this in (6) the steady state solution of drug in the SC for equal binding and unbinding rates and equal bound and unbound drug on the boundary is

$$\underline{C} = \alpha R_u \begin{bmatrix} 1 \\ 1 \\ 0 \end{bmatrix} \tag{10}$$

i.e. we expect no spatial dependence in the steady state reservoir concentration. The reservoir size per unit surface area of the skin is given as

$$S_u = \alpha R_u L = S_b. \tag{11}$$

*2.4. Reservoir Size*

The size of the unbound and bound reservoir $(S_u, S_b)$ at steady state can be found by integrating the steady state solution over $x$ between 0 and $L$ which gives:

$$S_u = \int_0^L C_u(x)\mathrm{d}x = \frac{a\mu L}{\gamma} + b\left(\frac{\mu + \lambda_+ v}{\gamma\lambda_+}\right)(\exp(\lambda_+ L) - 1) + c\left(\frac{\mu + \lambda_- v}{\gamma\lambda_-}\right)(\exp(\lambda_- L) - 1), \tag{12}$$

$$S_b = \int_0^L C_b(x)\mathrm{d}x = aL + \frac{b}{\lambda_+}(\exp(\lambda_+ L) - 1) - \frac{c}{\lambda_-}(\exp(\lambda_- L) - 1), \tag{13}$$

where $a, b, c$ are constants (7-9) and

$$\lambda_+ = \frac{\frac{v}{D} - \frac{\mu}{v} + \sqrt{\left(-\frac{v}{D} + \frac{\mu}{v}\right)^2 + 4\left(\frac{\mu}{D} + \frac{\gamma}{D}\right)}}{2}, \tag{14}$$

$$\lambda_- = \frac{\frac{v}{D} - \frac{\mu}{v} - \sqrt{\left(-\frac{v}{D} + \frac{\mu}{v}\right)^2 + 4\left(\frac{\mu}{D} + \frac{\gamma}{D}\right)}}{2}. \tag{15}$$

We use these expressions to explore how changes in model parameters affect reservoir size.

### *2.5. Parameter Values Used in Numerics*

The thickness of the SC (L) is dependent on many variables including region of the body, age, gender and health. In a study by Sandby et al [18] the average thickness of the SC for the forearm, where measurements are usually taken, is given as $18.3\mu m$ and it is this value chosen for $L$ in numerical simulations.

The time taken to renew the SC is typically taken to be 14 days for a healthy adult [19, 20, 16], we therefore take $v$ to be $0.054\mu m h^{-1}$.

Values of $D, \mu$ and $\gamma$ are drug dependent and are often uncertain or unknown. Boundary values $\alpha R_u$ and $\alpha R_b$ come from the first model and are consequently variable and depend on drug intake. We therefore explore the dependence of our reservoir size on these unknown parameters.

## 3. Results

### *3.1. Dependence of Reservoir Size on Binding*

The importance of binding parameters in transdermal drug delivery has been highlighted recently in a paper by Pontrelli and de Monte [21]. A comparison between reservoir size and diffusion coefficient, D, for different binding rates with different bound/unbound ratios at the boundary is given in Figure 4. From this we can see that for sufficiently large D reservoir size approaches a constant value dependent on the boundary conditions and binding rates. The relative proportion of bound to unbound drug in the reservoir at steady state appears to be controlled by the binding rates, $\gamma$ and $\mu$, whereas the scale of the reservoir is affected by a combination of the ratio of bound/unbound drug at the boundary and the rates of binding, $\gamma$, and unbinding, $\mu$ in the SC.

Next we explore how the reservoir size depends on the binding and unbinding rates whilst keeping D fixed and boundary conditions constant. In Figure 5(a) we vary $\gamma$ and observe that the total reservoir size increases essentially linearly with $\gamma$, driven by an increase in the amount of bound drug. Variation in $\gamma$ has no effect on the amount of unbound drug in the reservoir at steady state (due to the non-zero value of D). In Figure 5(b), we vary $\mu$ and in this case observe that the total reservoir size is inversely proportional to $\mu$, again driven by a similar relation between bound drug and $\mu$. From both graphs we see that binding mechanisms of drug within the SC may prove a crucial factor in expected reservoir size. Moreover the comparative levels of bound and unbound drug may be significant when considering extraction of the reservoir. If, for example, only unbound drug is retrieved with a given extraction method, high binding and low unbinding may decrease rather than increase observed reservoir size.

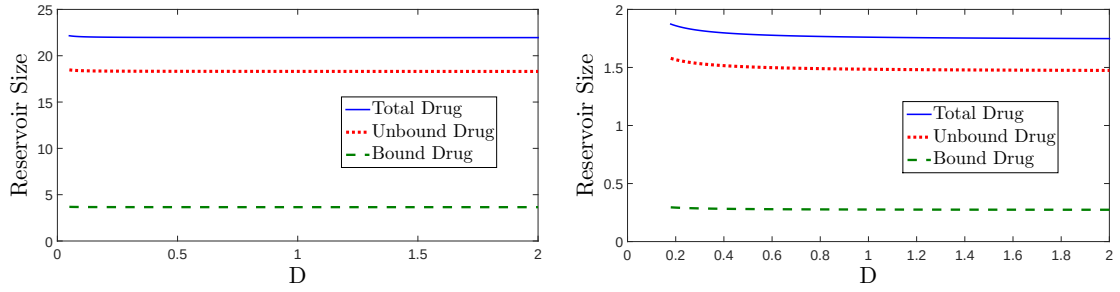


(a) $\mu$=5, $\gamma$=1, $\alpha R_u = \alpha R_b$=1 (b) $\mu$=5, $\gamma$=1, $\alpha R_u$=0.08 $\alpha R_b$=1.92

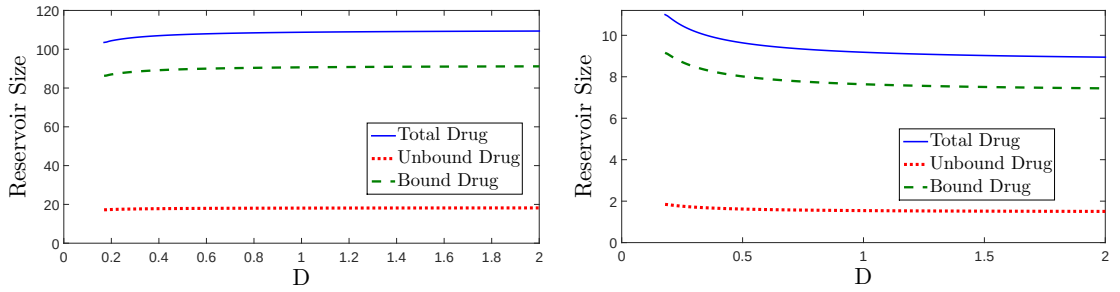


(c) $\mu$=1, $\gamma$=5, $\alpha R_u = \alpha R_b$=1 (d) $\mu$=1, $\gamma$=5, $\alpha R_u$=0.08 $\alpha R_b$=1.92

Figure 4: Steady state reservoir size plotted against D for the cases $\mu > \gamma$ with (a) even ($\alpha R_u = \alpha R_b = 1$) and (b) uneven ($\alpha R_u = 0.08, \alpha R_b = 1.92$) binding on the constant boundary at x=0 and for the case $\mu < \gamma$ with (c) even ($\alpha R_u = \alpha R_b = 1$) and (d) uneven ($\alpha R_u = 0.08, \alpha R_b = 1.92$) binding on the constant boundary at $x = 0$. As parameter values chosen here are for qualitative exploration, units of reservoir size have been omitted.

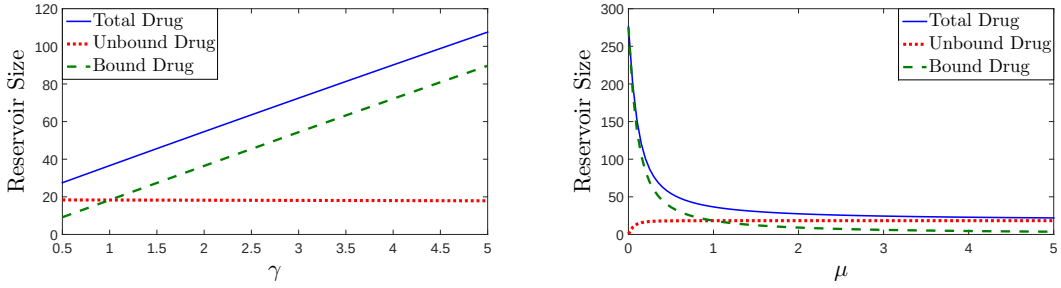


(a) $D = 0.5$, $\mu$=1, $\alpha R_u = \alpha R_b$=1 (b) $D = 0.5$, $\gamma$=1, $\alpha R_u = \alpha R_b$=1

Figure 5: Steady state reservoir size plotted against (a) binding rate, $\gamma$ with constant $\mu = 1$ and (b) unbinding rate $\mu$, with constant $\gamma = 1$ both graphs plotted using constant diffusion, $D = 0.5$ and constant boundary conditions at $x = 0$, $\alpha R_u = \alpha R_b = 1$. As parameter values chosen are for qualitative exploration, units of reservoir size have been omitted.

### *3.2. Dependence of Reservoir Size on Boundary Drug Distribution*

In Figure 6 we show how the binding ratio for drug in the poorly perfused tissue (Figure 2) impacts on reservoir size. From this figure we note that; in all cases, as the percentage of drug

that is unbound increases in body, the reservoir size increases and when the rate of binding exceeds the rate of unbinding in the SC, the reservoir size is significantly larger than when this relation is reversed. Again this has relevance for the extraction process as detailed above in 3.1.

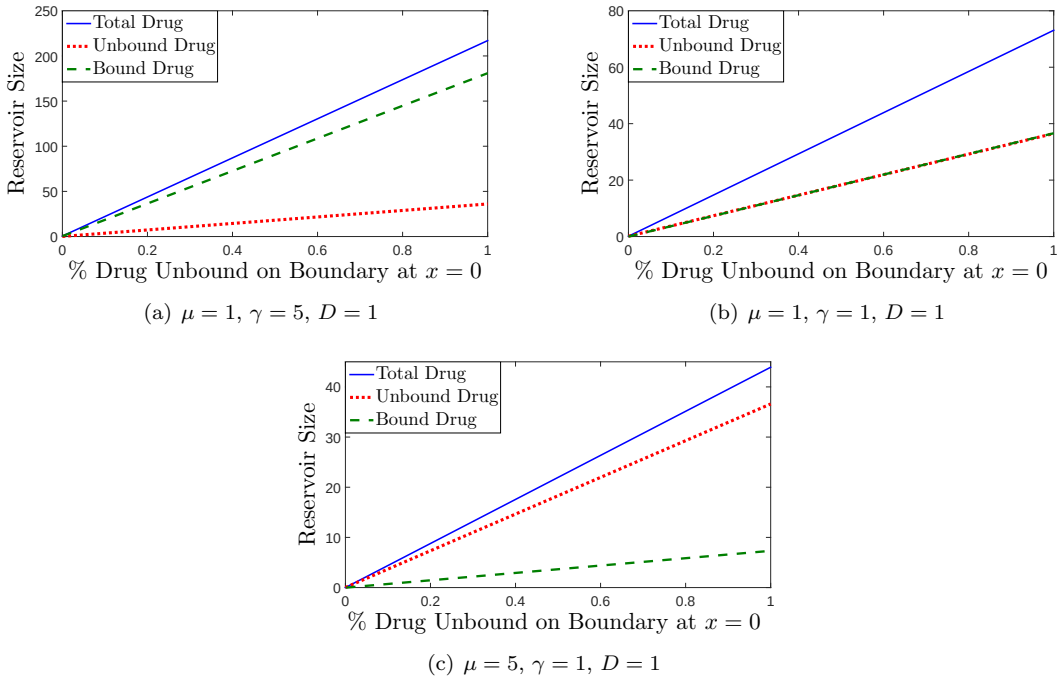


(a) $\mu = 1$, $\gamma = 5$, $D = 1$

(b) $\mu = 1$, $\gamma = 1$, $D = 1$

(c) $\mu = 5$, $\gamma = 1$, $D = 1$

Figure 6: Steady state reservoir size plotted against % of drug unbound on boundary $x = 0$ for constant total boundary condition $\alpha R_u + \alpha R_b$=2 for (a) $\mu > \gamma$ (b) $\mu = \gamma$ (c) $\mu < \gamma$. As parameter values chosen are for qualitative exploration, units of reservoir size have been omitted.

### *3.3. Time to Form Reservoir*

Whilst steady state reservoir size provides valuable information about the scale of the drug storage in the skin, it does not provide any information on how long it takes for the reservoir to form. This is an important measure as it indicates how sensitive the reservoir size is to a change in boundary condition and therefore how quickly it will reflect a change in dose.

In the case where the rate of unbinding is greater than the rate of binding ($\mu > \gamma$), illustrated by Figures 7(a) and 7(b), the time taken to reach steady state decreases with an increase in D, i.e. the faster the diffusion of unbound drug, the quicker the reservoir is to settle to its steady state level. For small D the accumulation of the reservoir is initially slower than for large D but over time this reverses. This is because initially, greater diffusion allows unbound drug to access the whole region before becoming bound and so the reservoir builds rapidly but as the unbound drug spreads through the region, having smaller diffusion allows more drug to become bound and hence the reservoir size increases.

In the case where the rate of binding is greater than the rate of unbinding ($\gamma > \mu$), Figure 7(c), 7(d), the time taken to reach steady state increases with an increase in D. This is because in this

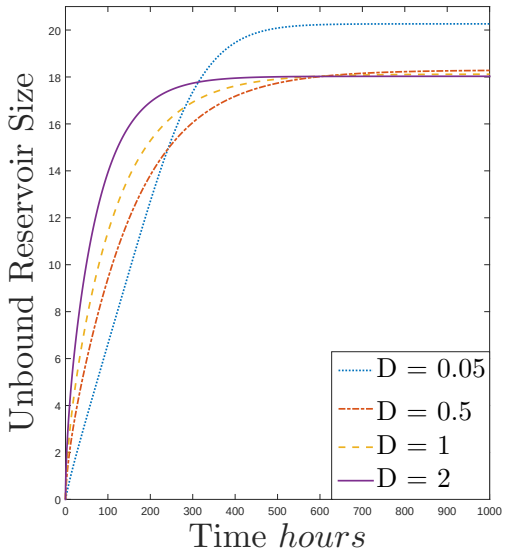


(a) $\mu = 2$, $\gamma = 1$

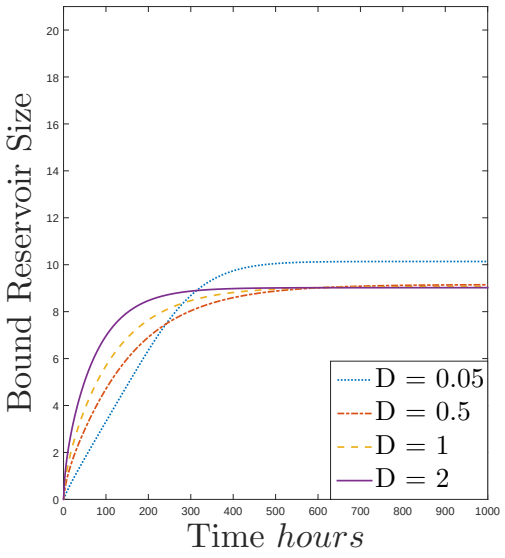


(b) $\mu = 2$, $\gamma = 1$

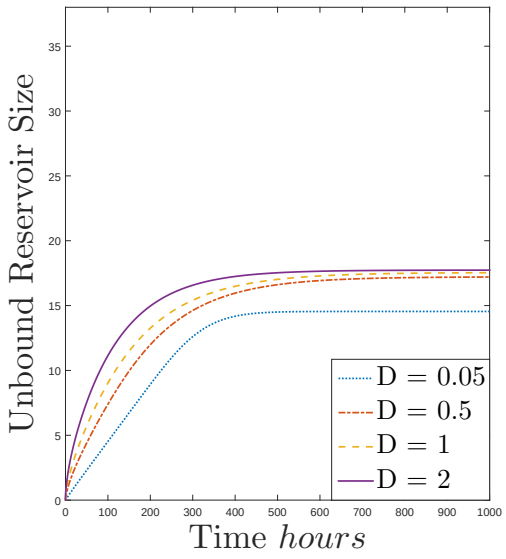


(c) $\mu = 1$, $\gamma = 2$

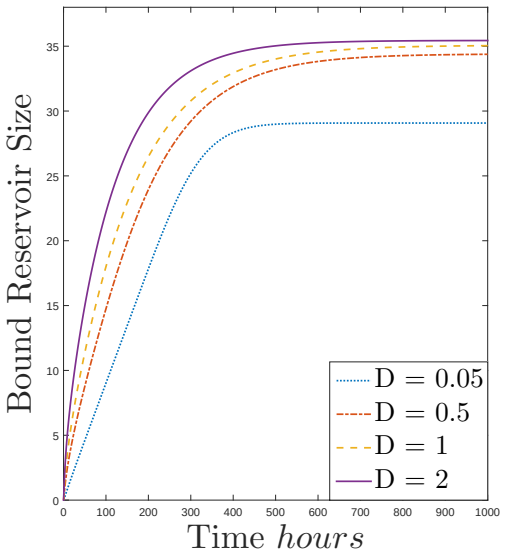


(d) $\mu = 1$, $\gamma = 2$

Figure 7: Reservoir size plotted against time for diffusion coefficient D= 0.05, 0.5, 1 and 2 with constant boundary conditions, $\alpha\bar{R}_u = \alpha\bar{R}_b = 1$ for a) unbound drug with unbinding rate ($\mu$) > binding rate ($\gamma$), b)bound drug with unbinding rate ($\mu$) > binding rate ($\gamma$), c)unbound drug with unbinding rate ($\mu$) < binding rate ($\gamma$), d)bound drug with unbinding rate ($\mu$) < binding rate ($\gamma$). As parameter values chosen are for qualitative exploration, units of reservoir size have been omitted.

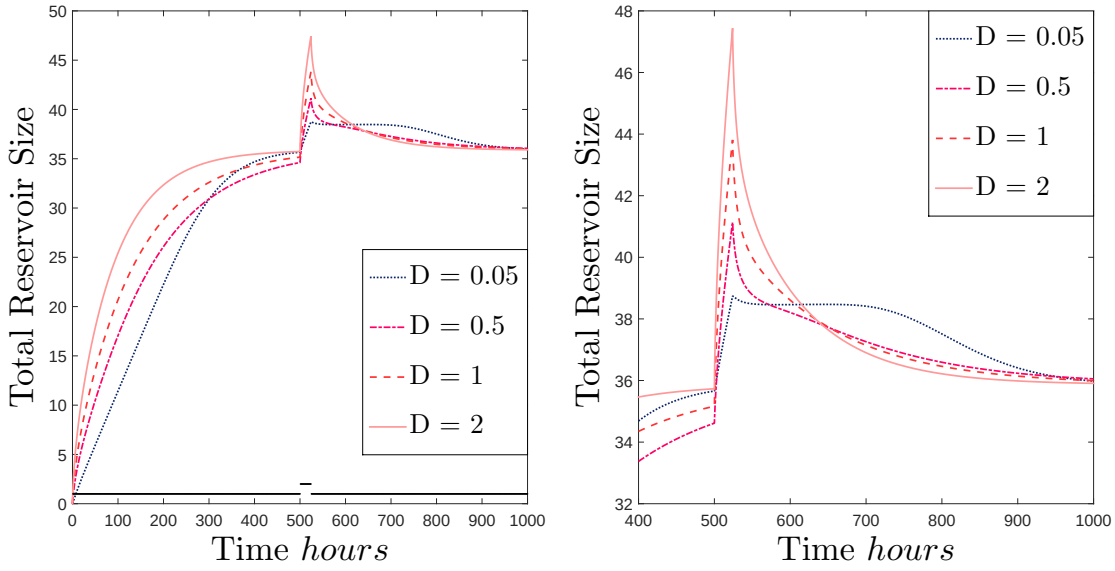


(a) (b)

Figure 8: a) Total reservoir size plotted against time for diffusion coefficient D= 0.05, 0.5, 1 and 2 with constant boundary conditions, $\alpha\bar{R_u} = \alpha\bar{R_b} = 1$ and equal binding and unbinding, $\mu = \gamma = 1$. with a perturbation to the boundary conditions at t=500h for 24 hours of $\alpha\bar{R_u} = \alpha\bar{R_b} = 2$. b) Enlarged view of Figure 8(a). As parameter values chosen are for qualitative exploration, units of reservoir size have been omitted.

case at steady state we expect more bound than unbound drug in the reservoir. The dominant equation in this case is therefore (3b). When D is sufficiently small, the governing equation for unbound drug (3a) is in agreement with the bound equation and both bound and unbound drug move through the domain with the skin ($v$) allowing for local binding dynamics to settle quickly and therefore reaching steady state quickly. However presence of diffusion in equation (3a) disrupts the system, with larger D values causing a greater perturbation and therefore taking longer to reach steady state.

In Figure 8(a) we show how quickly a perturbation to the drug concentrations at the boundary affects the reservoir size, depending on the diffusion coefficient. To explore this behaviour $\mu$, $\gamma$ are set to 1 so that the effect of differing binding rates does not influence our results and similarly we take $\alpha\bar{R}_u = \alpha\bar{R}_b = 1$ so that drug concentrations at the boundary $x = 0$ are equal. In this figure, at $t = 500h$ a perturbation is applied at the boundary for 24 hours, we see that for larger values of D, the effect of the perturbation is more pronounced than for small D values but that the time taken to return to a steady reservoir size is much less for large diffusion coefficients than small diffusion coefficients.

This will be of importance when considering a fluctuating boundary condition as we have in the body (from Model 1). A larger D would result in a shorter time to steady state (i.e. equilibrating with in body concentrations quickly) which means that the reservoir size would reflect changes in body concentration more dramatically; meaning traces of a fluctuation will also be removed more quickly. Whereas a smaller D would result in a reservoir that is less sensitive to in-body concentration fluctuations.

Note that choices of $\gamma$ and $\mu$ in the above figures are arbitrary. Figures shown are representative of the cases where $\mu > \gamma$ and $\gamma > \mu$ and similar profiles were obtained for other choices of these unknown parameters.

### *3.4. The Effect of Dose Compliance from Model 1 on Predicted Reservoir Size*

Fluctuations in the boundary concentrations represent changes in systemic levels of drug which in turn reflects a change in dose of drug and would ultimately indicate what level of noncompliance would be observable in terms of reservoir size.

In the compliant case, with a daily dose of drug, Figure 9(a), we find that for a drug naive patient, our model predicts a build up of drug in the SC over time which eventually levels off.

In the case of one missed dose at week five, figure 9(b), though the reduction in reservoir size is evident in the time profile shown here, it is unlikely that such a small percentage change would be observable experimentally, particularly at the low concentrations suggested here. Moreover, after a week of taking the correct dose the level of drug in the skin is renewed and reaches similar levels expected for a fully compliant scheme.

If we now consider habitual non compliance, demonstrated here as a single dose every other day, figure 9(c), we see a notable reduction in reservoir size which reaches half the level of the compliant case. This result is promising for potential compliance monitoring via the SC.

The time scales and values predicted rely on many uncertain parameter values for both in body and in skin models. In order to get a better idea of how much drug reaches the SC and how quickly the reservoir changes, more data are needed.

## 4. Conclusion

A two model system has been developed and analysed which describes the relationship between a drug reservoir in the SC and drug concentration in the body. It follows work by Paulley et al

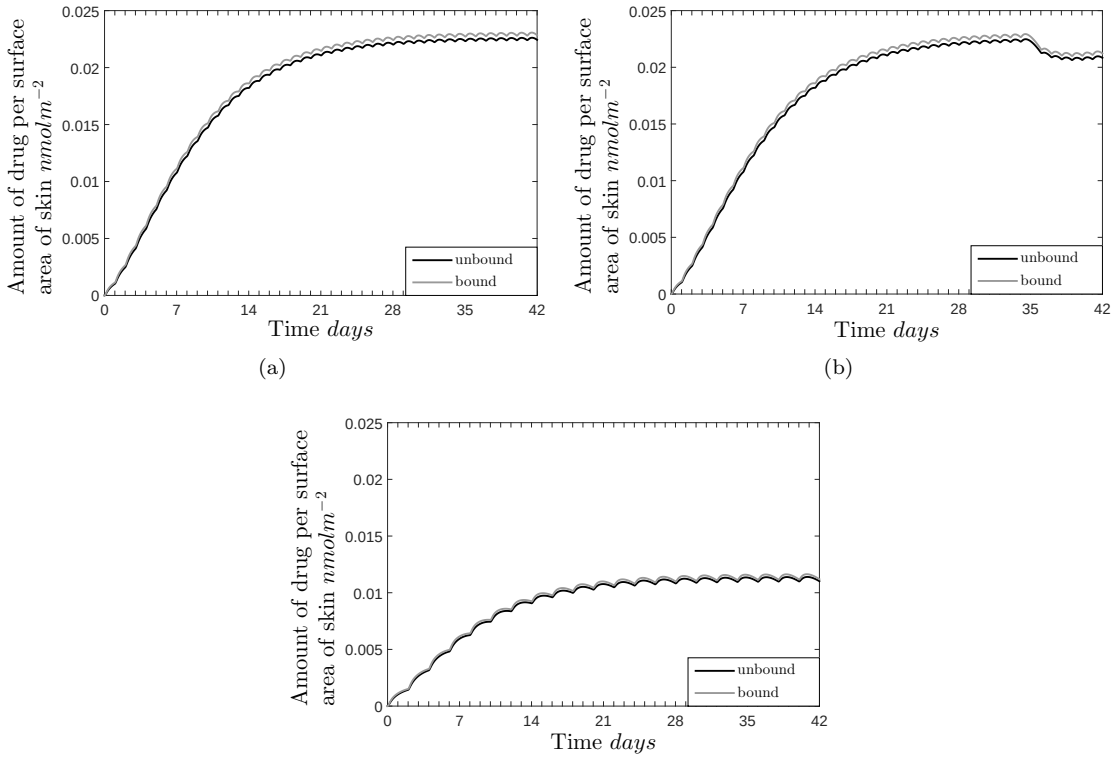


Figure 9: Simulation of SC reservoir build-up of bound and unbound drug for a) a single daily dose for 6 weeks in drug- naive patient, b) a single daily dose for 6 weeks with one missed dose at the begining of week 5 in drug-naive patient, c) a single dose every other day for 6 weeks in drug- naive patient. Using 'poorly perfused tissue' compartment from model 2 for systemic concentration as boundary conditions for SC model 3.

[10] which used mathematical modelling to support observations that lithium reservoirs form when drug is administered for chronic illness. The model presented here extends those ideas to the case where the drug is found in both bound and unbound forms and in which the lipophilicity of the drug are considered. Buprenorphine is used as an exemplar drug to populate some of the model parameter values in numerical simulations.

Analysis has highlighted the importance of binding and unbinding in creating a reservoir of a size that might reasonably be observed in the laboratory, this supports the findings by Pontrelli and de Monte [21]. It has also provided insight into the time scales associated with reservoir formation and response to in-body changes in drug concentration. The modelling highlights the need to undertake experimental work to obtain parameter estimates; if these can be obtained, then we have created a highly customisable structure which could be exploited to predict drug reservoir levels and the impact which perturbations to drug regimens will have on this measure. Moreover, the system lends itself well to the exploration of non-invasive extraction and drug monitoring techniques across the skin as it describes both total amount in the SC and also spatial distribution of drug in the SC. The first measure is relevant to extraction techniques such as reverse iontophoresis whilst the second lends itself to the process of tape stripping.

Of course, the model has limitations. It provides a very simplified structure for drug distribution in the body and also movement of drug in the lipid matrix of the SC. However at this stage, it still provides useful insight into how a drug reservoir may establish depending on key drug properties such as binding affinity. Another issue may be interpatient variability such as age and ethnicity which could be incorporated by careful modification of 'average' model parameter estimates once such data sources are available.

In the meantime, we believe that the results extracted from our model analysis can contribute to on going discussions about drug reservoirs in the skin, their dependence on the molecular properties of those drugs and the potential to exploit these reservoirs to improve drug monitoring techniques for chronically ill patients.

## 5. Acknowledgements

J.G.Jones is supported by the Engineering and Physical Sciences Research Council (EPSRC) studentship.

## Appendix A. Steady State Distributions in the Stratum Corneum

We define

$$\underline{C} = \begin{bmatrix} C_u \\ C_b \\ \omega \end{bmatrix} \tag{A.1}$$

with $\omega = \dfrac{dC_u}{dx}$ and use this to rewrite (3) at steady state as

$$\begin{bmatrix} \dot{C_u} \\ \dot{C_b} \\ \dot{\omega} \end{bmatrix} = \begin{bmatrix} 0 & 0 & 1 \\ \dfrac{\gamma}{v} & -\dfrac{\mu}{v} & 0 \\ \dfrac{\gamma}{D} & -\dfrac{\mu}{D} & \dfrac{v}{D} \end{bmatrix} \begin{bmatrix} C_u \\ C_b \\ \omega \end{bmatrix} \tag{A.2}$$

The eigenvalues of the system are

$$\lambda_0 = 0 \tag{A.3}$$

$$\lambda_+ = \frac{\frac{v}{D} - \frac{\mu}{v} + \sqrt{\left(-\frac{v}{D} + \frac{\mu}{v}\right)^2 + 4\left(\frac{\mu}{D} + \frac{\gamma}{D}\right)}}{2} \tag{A.4}$$

$$\lambda_- = \frac{\frac{v}{D} - \frac{\mu}{v} - \sqrt{\left(-\frac{v}{D} + \frac{\mu}{v}\right)^2 + 4\left(\frac{\mu}{D} + \frac{\gamma}{D}\right)}}{2} \tag{A.5}$$

with corresponding eigenvectors

$$\underline{\mathrm{v}}_0 = \begin{bmatrix} \frac{\mu}{\gamma} \\ 1 \\ 0 \end{bmatrix}, \underline{\mathrm{v}}_+ = \begin{bmatrix} \frac{\mu + \lambda_+ v}{\gamma} \\ 1 \\ \frac{\lambda_+ \mu + {\lambda_+}^2 v}{\gamma} \end{bmatrix}, \underline{\mathrm{v}}_- = \begin{bmatrix} \frac{\mu + \lambda_- v}{\gamma} \\ 1 \\ \frac{\lambda_- \mu + {\lambda_-}^2 v}{\gamma} \end{bmatrix} \tag{A.6}$$

**Appendix B.**

| Parameter | Description | Range | Value used in numerics | Calculation | Relevant data w/ references |
|---|---|---|---|---|---|
| $k_1$ | Rate of binding of bup in plasma ($h^{-1}$) | $k_1 >> k_2$ | 1000 | | |
| $k_2$ | Rate of movement between plasma and well perfused tissues ($h^{-1}$) | $k_2 > k_3$, | 0.5 | | |
| $k_3$ | Rate of movement between plasma and poorly perfused tissues ($h^{-1}$) | $k_2 > k_3$, | 0.1 | | |
| $k_4$ | Rate of excretion of bup ($h^{-1}$) | | 0.30 | | Mean Value of elimination rate constant estimated for 1.2mg IV [22] |
| $k_5$ | rate of binding of bup in well perfused tissues ($h^{-1}$) | | 100 | | |
| $k_6$ | Rate of binding of bup in poorly perfused tissues ($h^{-1}$) | | 100 | | |
| $V_{max}$ | Max velocity (michaelis menten kinetics for bup metabolism) ($\mu moll^{-1}h^{-1}$) | 829<br><br><br><br><br><br>(3.62-4.04 x $10^3$) | 829 | 0.712(Vmax) x 32(MPPGL) x1820(liver weight) x 60(min− >hr) x $10^{-9}$(nmol) /3L(plasma vol) | 0.712nmol $min^{-1}$mg of $protein^{-1}$[23]<br>$MPPGL = 32mg/g$ [24]<br>liver weight= 2.6% of BW [25]<br>70kg human<br><br><br>($3.14 \pm 0.033$nm $min^{-1}$mg$protein^{-1}$[26]) |
| $k_m$ | Michaelis rate constant for bup ($\mu moll^{-1}$) | 39.3 ±9.2<br>(85 ± 16 ) | 39.3 | | $39.3 \pm 9.2 \mu Molar$[23]<br>( $85 \pm 16 \mu Molar$[26]) |
| $f_{up}$ | Fraction of bup in plasma unbound | 0.04 | 0.04 | - | [27] |
| $f_{uq}$ | Fraction of bup in well perfused tissues that is unbound | [0,1] | 0.04 | see text | |
| $f_{ur}$ | Fraction of bup in poorly perfused tissues that is unbound | [0,1] | 0.04 | see text | |
| $f_2$ | Ratio of unbound bup between plasma and well perfused tissues at equilibrium | $f_2 > f_3$ | 0.5 | see text | |
| $f_3$ | Ratio of unbound bup between plasma and poorly perfused tissues at equilibrium | $f_2 > f_3$ | 0.2 | see text | |
| $k$ | absorption constant ($h^{-1}$) | | 2.5 | | |
| $\delta$ | Sublingual dose of bup ($\mu moll^{-1}$)<br>Intravenous dose of bup | dose (mg) x 0.3394<br><br>dose (mg) x 0.6789 | 0.431 | $\frac{\text{dose x bioavailability}}{\text{M x plasma vol}}$ | sublingual bioavaliability= 50% [28]<br>molar mass (M)= 467.64<br>plasma vol= 3.15L [12] |
| $V_{Q/P}$ | ratio of volumes of well perfused tissue and plasma compartments | | 3.18 | 10.031/3.15 | $V_Q$= 10.031 L[12, 29] |
| $V_{R/P}$ | ratio of volumes of poorly perfused tissue and plasma compartments | | 17.6 | 55.51/3.15 | $V_R$ = 55.51 L [12, 29] |

Table B.1: parameters and their estimates along with calculations and appropriate data sources.

[1] M. S. Roberts, S. E. Cross, and Y. G. Anissimov, "Factors affecting the formation of a skin reservoir for topically applied solutes," *Skin Pharmacology and Physiology*, vol. 17, pp. 3–16, 2004.

[2] C. H. Vickers, "Existence of reservoir in the stratum corneum: Experimental proof," *Archives of Dermatology*, vol. 88, no. 1, pp. 20–23, 1963.

[3] R. D. Carr and R. G. Wieland, "Corticosteroid reservoir in the stratum corneum," *Archives of Dermatology*, vol. 94, no. 1, pp. 81–84, 1966.

[4] C. H. Vickers, "Stratum corneum reservoir for drugs," *Advances in Biology of Skin*, vol. 12, pp. 177–189, 1972.

[5] J. M. Nitsche and H. F. Frasch, "Dynamics of diffusion with reversible binding in microscopically heterogeneous membranes: General theory and applications to dermal penetration," *Chemical Engineering Science*, vol. 66, no. 10, pp. 2019 – 2041, 2011.

[6] M. B. Reddy, R. H. Guy, and A. L. Bunge, "Does epidermal turnover reduce percutaneous penetration?," *Pharmaceutical Research*, vol. 17, no. 11, pp. 1414–1419, 2000.

[7] S. Seif and S. Hansen, "Measuring the stratum corneum reservoir: Desorption kinetics from keratin," *Journal of Pharmaceutical Sciences*, vol. 101, pp. 3718–3728, 2012.

[8] B. Leboulanger, J. Aubry, G. Bondolfi, R. H. Guy, and B. M. Delgado-Charro, "Lithium monitoring by reverse iontophoresis in vivo," *Clinical Chemistry*, vol. 50, no. 11, pp. 2091–2100, 2004.

[9] B. Leboulanger, M. Fathi, R. Guy, and B. M. Delgado-Charro, "Reverse iontophoresis as a non-invasive tool for lithium monitoring and pharmacokinetic profiling," *Pharmaceutical Research*, vol. 21, no. 7, pp. 1214–1222, 2004.

[10] Y. Paulley, M. B. Delgado-Charro, and K. A. J. White, "Modelling formation of a drug reservoir in the stratum corneum and its impact on drug monitoring using reverse iontophoresis.," *Computational and Mathematical Methods in Medicine*, vol. 11, no. 4, p. 353, 2010.

[11] A. Rostami-Hodjegan, "Physiologically based pharmacokinetics joined with in vitro- in vivo extrapolation of adme: A marriage under the arch of systems pharmacology," *Clinical Pharmacology and Therapeutics*, vol. 92, no. 1, 2012.

[12] A. Paradkar, *Biopharmaceutics & Pharmacokinetics*, ch. 3. Pragati Books, 2008.

[13] *Modeling in Biopharmaceutics, Pharmacokinetics, and Pharmacodynamics: Homogeneous and Heterogeneous Approaches*. Springer Science and Business Media, Inc., New York, 2006.

[14] Y. G. Anissimov and M. S. Roberts, "Diffusion modelling of percutaneouos absorption kinetics:4. effects of a slow equilibration process within stratum corneum on absorption and desorption kinetics," *Journal of Pharmaceutical Sciences*, vol. 98, pp. 772–781, 2008.

[15] A. C. Williams, *Transdermal and Topical Drug Delivery*. Pharmaceutical Press, 2003.

[16] L. Jansen, M. Hojyotom, and A. Kligman, "Improved fluorescence staining technique for estimating turnover of human stratum-corneum," *British Journal of Dermatology*, vol. 90, no. 1, pp. 9–12, 1974.

[17] L. Simon, K. Kwang, and K. Kanneganti, "Effects of epidermal turnover on the dynamics of percutaneous drug absorption," *Mathematical Biosciences*, vol. 229, pp. 16–21, 2011.

[18] J. Sandby-Moller, T. Poulsen, and H. C. Wulf, "Epidermal thickness at different body sites: Relationship to age, gender, pigmentation, blood content, skin type and smoking habits," *Acta Dermato- Venereologica*, vol. 83, pp. 410–413, 2003.

[19] S. Rotheberg, R. Crounse, and J. Lee, "Glycine-c-14 incorporation into the proteins of normal stratum corneum and the abnormal stratum corneum of psoriasis," *Journal of Investigative Dermatology*, vol. 37, no. 6, pp. 497–505, 1961.

[20] G. Weinstei and E. Vanscott, "Autoradiographic analysis of turnover times of normal and psoriatic epidermis," *Journal of Investigative Dermatology*, vol. 45, no. 4, p. 257, 1965.

[21] G. Pontrelli and F. de Monte, "A two-phase two-layer model for transdermal drug delivery," *Mathematical Biosciences*, vol. 257, pp. 96–103, 2014.

[22] J. J. Kuhlman, S. Lalani, J. Magluilo, B. Levine, W. D. Darwin, R. E. Johnson, and E. J. Cone, "Human pharmacokinetics of intravenous, sublingual, and buccal buprenorphine," *Journal of Analytical Toxicology*, vol. 20, pp. 369–378, 1996.

[23] K. Kobayashi, T. Yamamoto, K. Chiba, M. Tani, N. Shimada, T. Ishizaki, and Y. Kuroiwa, "Human buprenorphine N-dealkylation is catalyzed by cytochrome P450 3A4," *Drug Metabolism and Disposition*, vol. 26, no. 8, pp. 818–821, 1998.

[24] Z. E. Barter, J. E. Chowdry, J. R. Harlow, J. E. Snawder, J. C. Lipscomb, and A. Rostami-Hodjegan, "Covariation of human microsomal protein per gram of liver with age: Absence of influence of operator and sample storage may justify interlaboratory data pooling," *Drug Metabolism and Disposition*, vol. 36, no. 12, pp. 2405–2409, 2008.

[25] G. L. Kedderis and S. D. Held, "Prediction of furan pharmacokinetics from hepatocyte studies: Comparison of bioactivation and hepatic dosimetry in rats, mice, and humans," *Toxicology and Applied Pharmacology*, vol. 140, no. 1, pp. 124 – 130, 1996.

[26] C. Iribarne, D. Picart, Y. Dreano, J.-P. Bail, and F. Berthou, "Involvement of cytochrome P450 3A4 in N-dealkylation of buprenorphine in human liver microsomes," *Life Sciences*, vol. 60, no. 22, pp. 1953–1964, 1997.

[27] R. Heel, R. Brogden, T. Speight, and G. Avery, "Buprenorphine: A review of its pharmacological properties and therapeutic efficacy," *Drugs*, vol. 17, no. 2, pp. 81–110, 1979.

[28] R. P. Nath, R. A. Upton, E. T. Everhart, P. Cheung, P. Shwonek, R. T. Jones, and J. E. Mendelson, "Buprenorphine pharmacokinetics: Relative bioavailability of sublingual tablet and liquid formulations," *The Journal of Clinical Pharmacology*, vol. 39, pp. 619–623, 1999.

[29] P. Poulin and S. Haddad, "Advancing prediction of tissue distribution and volume of distribution of highly lipophilic compounds from a simplified tissue-composition-based model as a mechanistic animal alternative method," *Journal of Pharmaceutical Sciences*, vol. 101, no. 6, pp. 2250–2261, 2012.